Comparative Analysis of the Morphology, Ultrastructure, and Glycosylation Pattern of the Jejunum and Ileum of the Wild Rodent *Lagostomus maximus*

MARÍA FLORENCIA TANO DE LA HOZ,[1,2] MIRTA ALICIA FLAMINI,[3] AND ALCIRA OFELIA DÍAZ[2]*

[1]Consejo Nacional de Investigaciones Científicas y Técnicas (CONICET), Argentina
[2]Instituto de Investigaciones Marinas y Costeras (IIMyC), Departamento de Biología, FCEyN, CONICET-Universidad Nacional de Mar del Plata, Funes 3250 3° piso, 7600 Mar del Plata, Argentina
[3]Departamento de Histología y Embriología, Facultad de Ciencias Veterinarias, Universidad Nacional de La Plata, La Plata 1900, Argentina

ABSTRACT

Morphological and histochemical analyses were performed to characterize the histology, ultrastructure, and glycosylation pattern of the jejunum and ileum of the wild rodent *Lagostomus maximus*. Enterocytes, goblet cells, Paneth cells, and enteroendocrine cells were identified in both intestinal epithelia. Two morphological types of enterocytes were identified only in the ileum based on their cytoplasm electron density. Although the histological and ultrastructural examination showed that the epithelia of both anatomical regions were morphologically similar, a certain specialization in their secretory products was evident. The glycosylation pattern of the jejunum and ileum was characterized *in situ* by histochemical and lectin histochemical methods. Histochemical results revealed the presence of carboxylated and sulfated gycoconjugates in both regions, although sulfomucins were clearly prevalent in the ileum. Sialic acid was highly O-acetylated and particularly abundant in the jejunum. The KOH/PA*/Bh/PAS technique evidenced a more intense histochemical reaction in the jejunal than in the ileum goblet cells, demonstrating a reduction of neutral mucin secretion in the distal small intestine. Further specific differences were revealed by lectin histochemistry. These data evidenced that the nature of mucus varies at different anatomical regions, probably adapted to physiological requirements. Anat Rec, 299:630–642, 2016. © 2016 Wiley Periodicals, Inc.

Key words: *Lagostomus maximus*; small intestine; ultrastructure; morphology; glycopattern analysis

Grant sponsor: National University of Mar del Plata, Buenos Aires, Argentina.

*Correspondence to: A.O. Díaz; Instituto de Investigaciones Marinas y Costeras (IIMyC), FCEyN, CONICET-Universidad Nacional de Mar del Plata. Funes 3250 3° piso, 7600 Mar del Plata, Buenos Aires, Argentina. Fax: +54-223-4753150.
E-mail: adiaz@mdp.edu.ar

Received 22 September 2015; Revised 12 January 2016; Accepted 26 January 2016.

DOI 10.1002/ar.23335
Published online 24 February 2016 in Wiley Online Library (wileyonlinelibrary.com).

INTRODUCTION

The gastrointestinal tract of mammals is subjected to permanent mechanical as well as chemical injuries caused by the ingested food. Moreover, the emptying of digestive enzymes, hydrochloric acid, and bile acids creates a highly hostile environment for the simple columnar epithelium (Bansil and Turner, 2006). The gastrointestinal epithelial cells are protected at least by a mucus layer, mainly composed of water and mucins, and minor components such as electrolytes (Neutra and Forstner, 1987; Moran et al., 2011).

Intestinal mucins are principally synthesized by goblet cells and they occur both as soluble-secreted and membrane-bound forms. Mucins are glycoproteins (GPs) with a high content of O-linked oligosaccharides and a less proportion of N-linked oligosaccharides (Bansil and Turner, 2006). They play different functional roles such as lubricating and protecting the epithelial cells from mechanical and chemical abrasion. In addition, they also provide attachment site for commensal and pathogenic microbes (Robbe et al., 2004; Kim and Ho, 2010). Glycoproteins are characterized by an elevated content of carbohydrate which defined their high molecular weights and a large part of their physicochemical features (Liquori et al., 2012).

At present, there are scarce studies that analyze the histochemical profile of normal mammalian gut and little is known about the glycosylation pattern throughout the gastrointestinal tract.

Recent studies on mammals have shown that both the distribution of goblet cells and the mucin subtypes vary spatially as well as temporally all along the gastrointestinal tract, and according to specific factors such as animal species, age, position along crypt-villus axis, diet, and bacterial status (Beyaz and Liman, 2009; Liquori et al., 2012; Mastrodonato et al., 2013; Tano de la Hoz et al., 2014).

The plains viscacha (*Lagostomus maximus*), a Hystricognathi rodent (Rodentia, Caviomorpha) of the Chinchillidae family, inhabit a wide zone of the Argentine territory. This is a species of zootechnical interest due to the profitableness of its leather and the nutritional value of its meat (Jackson, 1985). In that regard, since the last decade, the South American as well as the African histricomorph rodents have occupied an important place in international plans of promotion of sustainable development (Edderai et al., 2001; Addo et al., 2003), being suggested for its inclusion in international economic development programs, and in basic and applied sciences (National Research Council, 2000). Despite this interest, researches on the digestive system's morphology of *L. maximus* are scarce (Llanos and Crespo, 1952) and little is known about the histochemical and physiological aspects of the intestinal epithelium (Tano de la Hoz et al., 2014).

The aim of this study focused on the comparative analysis in morphology, ultrastructure, and glycosylation pattern of the jejunum and ileum of *L. maximus*. For this purpose, the ultrastructural features of the different epithelial cells types of the jejunum and ileum were analyzed by transmission electron microscopy. Moreover, histochemical and lectin-histochemical techniques were used to characterize *in situ* the glycosylation pattern of the intestinal epithelial cells so as to analyze the variation in the distribution of mucins and its possible physiological role.

MATERIALS AND METHODS

Animals

Six *L. maximus* wild adults of both sexes, 3–5 kg body weight, were used. Animals were captured in the Buenos Aires province (Argentina) with strategically built traps set at the entrance of their caves. Clinical and pathological examinations in all animals confirmed that there were no signs of disorder.

Captured animals were anesthetized by intramuscular injection of xylacine (8 mg/kg body weight) followed by ketamine (50 mg/kg body weight) (Ketanest, Laboratorio Scott Cassara). Once at deep plane of anesthesia, intracardiac perfusion with a physiological saline solution and afterward with 4% paraformaldehyde in 0.1 M buffer phosphate was performed. The method was carried out according to the international recommendations for the use of research animals (Commission on Life Sciences National Research Council, 1996; Zuñiga et al., 2001).

Sampling

The necropsy was carried out immediately after sacrifice by taking samples of jejunum and ileum. Samples were routinely processed and embedded in paraffin wax. Histological sections of 4 μm thickness were cut by microtome and prepared according to standard protocol. For the observation of general histology, sections from each tissue block were stained with hematoxylin and eosin (H–E) and Masson trichrome stain. Micrographs were taken with an Olympus microscope, CH30 (Olympus; www.olympus.com).

Ultrastructural Study

For transmission electron microscopy (TEM), the jejunum and ileum of three *L. maximus* wild adults were analyzed. Sections of 0.5–1 mm side length from both anatomical regions were obtained. Sections were fixed in cold (4°C) 3% glutaraldehyde in 0.1 M cacodylate buffer at pH 7.3 for 24 h, rinsed in 0.01 M phosphate-buffered saline (PBS), pH 7.2 for 30 min and sent to the Electron Microscopy Laboratory, School of Veterinary Sciences, National University of La Plata. There, the samples were postfixed in cold (4°C) 1% osmium tetroxide for 1 h, dehydrated in a graded ethanol series, and embedded in Epoxy resin (Epok 812). Semithin sections were stained with Toluidine Blue and observed by light microscopy to select fields. Ultrathin sections were mounted on copper grids, double-stained with uranyl acetate and lead citrate, examined in a JEOL JEM 1200 EX II electron microscope, and shot with a digital camera (ES 500W Erlangshen CCD Gatan).

Traditional Histochemistry

Sections of tissue were also subjected to histochemical procedures for glycoconjugates (GCs) identification, as detailed in Table 1. Sections were stained with (1) PAS (periodic acid-Schiff's reagent) to demonstrate periodate-reactive vicinal diols and glycogen; (2) α-amylase

TABLE 1. Histochemical techniques used

Procedures	Interpretation of staining reactions	References
1. PAS	GCs with oxidizable vicinal diols and glycogen	McManus (1948)
2. α-amylase-PAS	GCs with oxidizable vicinal diols	Pearse (1985)
3. KOH/PA*S	GCs with sialic acid residues	Culling et al. (1976)
4. PA/Bh/KOH/PAS	Sialic acid residues with O-acyl substitution at ^{7}C, ^{8}C, or ^{9}C and O-acyl sugars	Reid et al. (1973)
5. KOH/PA*/Bh/PAS	GCs with oxidizable vicinal diols and O-acyl sugars	Volz et al. (1987)
6. AB pH 2.5	GCs with carboxyl groups and O-sulfate esters	Lev and Spicer (1964)
7. AB pH 1.0	GCs with O-sulfate esters	Lev and Spicer (1964)
8. AB pH 0.5	Highly sulfated GCs	Lev and Spicer (1964)
9. AB pH 2.5/PAS	Same as in 6 and 1	Mowry (1963)
10. TB pH 5.6	GCs with O-sulfate esters and carboxyl groups	Lison (1953)
11. TB pH 4.2	GCs with O-sulfate esters	Lison (1953)

AB, Alcian blue; Bh, borohydride; PA*, selective periodic acid oxidation; PAS, periodic acid Schiff reagent; PA*S, periodic acid/Schiff at low temperature and low pH (oxidation with 0.4 mM periodic acid in 1.0 M hydrochloric acid at 4°C); TB, toluidine blue.

TABLE 2. Lectins used and their carbohydrate specificities

Lectin	Acronym	Specificity	Haptene
GROUP I		Glc/Man	
Canavalia ensiformis agglutinin	Con-A	α-D-Man; α-D-Glc	α-D-Methyl-Man
GROUP II		GlcNAc	
Triticum vulgaris (wheatgerm) agglutinin	WGA	β-D-GlcNAc; NeuNAc	NeuNAc
GROUP III		GalNAc/Gal	
Dolichos biflorus agglutinin	DBA	α-D-GalNAc	D-GalNAc
Glycine maximus agglutinin	SBA	α-D-GalNAc; β-D-GalNAc	D-GalNAc
Ricinus communis agglutinin-I	RCA-I	β-Gal	Lactose
Arachis hypogaea agglutinin	PNA	β-D-Gal (β1–3) > D-GalNAc	Lactose
GROUP IV		L-Fuc	
Ulex europaeus agglutinin-I	UEA-I	α-L-Fuc	L-Fuc

Gal, galactose; GalNAc, N-acetylgalactosamine; Glc, glucose; GlcNAc, *N*-acetylglucosamine; L-Fuc, L-fucose; Man, mannose; α-D-Methyl-Man, α-D-Methyl-mannose; NeuNAc, acetyl-neuraminic acid (sialic acid).

digestion before PAS reaction for a control of GCs presence with oxidizable vicinal diols; and (3) KOH/PA*S (saponification-selective periodic acid-Schiff reaction) to allow the characterization of total sialic acid. The saponification with 0.5% potassium hydroxide in 70% ethanol for 30 min at room temperature was performed to deacetylate sialic acid residues and was followed by PA*S; (4) PA/Bh/KOH/PAS (periodic acid–borohydride reduction–saponification–periodic acid-Schiff reaction): this method was carried out using a 2 h oxidation at room temperature with 1% periodic acid (PA). The aldehydes generated by the initial oxidation were reduced to Schiff-unreactive primary alcohols with sodium borohydride (Bh). Following saponification (KOH), only sialic acids with O-acyl substituents at C7, C8, or C9 (or which had two or three side-chains O-acyl substituents) were PAS positive; (5) KOH/PA*/Bh/PAS (saponification-selective periodic acid–borohydride reduction–periodic acid-Schiff reaction) for neutral sugar characterization; (6) AB pH 2.5 (Alcian Blue 8GX pH 2.5) to demonstrate GCs with carboxyl groups (sialic acid or uronic acid) and/or with O-sulfate esters; (7) AB pH 1.0 (Alcian Blue 8GX pH 1.0) to demonstrate GCs with O-sulfate esters; (8) AB pH 0.5 (Alcian Blue 8GX pH 0.5) to demonstrate highly sulfated GCs; (9) AB pH 2.5/PAS (Alcian Blue 8GX pH 2.5/periodic acid-Schiff staining) to differentiate between neutral and acidic carbohydrates in the same section; (10) TB pH 5.6 (toluidine blue) to demonstrate GCs with O-sulfate esters and carboxyl groups; (11) TB pH 4.2 (toluidine blue) to demonstrate GCs with O-sulfate esters.

Evaluation of labeling intensities was assessed by two independent observers and classified as: negative (0), weak (1), moderate (2), and strong (3). This classification was established according to previous reports (Liquori et al., 2012; Boonzaier et al., 2013; Mastrodonato et al., 2013).

Lectin Histochemistry

Labeling with biotinylated lectins was used to identify specific sugar residues of GCs. Seven different specific lectins, purchased at Vector Laboratories, Inc. (Burlingame, CA, USA), were employed (Table 2). Paraffin-embedded sections mounted on slides coated with Poly-L-lysine (Sigma Diagnostics, St Louis, MO, USA) were deparaffinized with xylene, incubated in 0.3% H_2O_2 (100 volumes) in methanol for 30 min at room temperature to block endogenous peroxidase activity, hydrated, and washed in 0.01 M phosphate-buffered saline (PBS), pH 7.2 and treated with 0.1% bovine serum albumin in PBS for 15 min to inhibit the nonspecific binding. Sections were incubated with biotinylated lectins for 30 min at room temperature and rinsed in PBS for 15 min and treated with avidin biotin–peroxidase complex (ABC) for 45 min (Vector Laboratories, Inc). The horseradish peroxidase was activated by incubation for 4–10 min with a buffered 0.05 M Tris–HCl pH 7.6 solution containing

0.02% diaminobenzidine (DAB) (Dako, Carpinteria, CA, USA) and 0.05% H_2O_2. Each lectin was used at a 30 μg/mL dilution in PBS, except for PNA, which was applied at a concentration of 10 μg/mL. Two types of controls were performed: (i) lectin solution was replaced by PBS and (ii) lectin labeling was performed as described previously after lectin preincubation for 1 h in the presence of the appropriate hapten sugars (0.2 Min PBS), as listed in Table 2, at room temperature. The intensity of the lectin histochemical staining was evaluated using the same semiquantitative scale that was used for histochemical analysis.

RESULTS

Histological and Ultrastructural Study

Goblet cells, enterocytes, enteroendocrine cells, and Paneth cells were recognized in the epithelium of the jejunum and ileum. Enterocytes were pronouncedly polar, exhibiting structural differences between the apical and basal part of the cell. The apical surface showed uniform and regular microvilli. Another cytological feature seen in these absorptive cells was the presence of junctional complexes between neighboring epithelial cells (Fig. 1A). The cytoplasm presented numerous ribosomes, cisterns of rough endoplasmic reticulum, a perinuclear Golgi apparatus, and apical aggregations of mitochondria (Fig. 1A–C). Based on the cytoplasm electron density, two morphological types of enterocytes were recognized only in the ileum; the more numerous cell type had electron-lucid cytoplasm while the lesser one had an electron-dense cytoplasm (Fig. 1D). Both electron-lucid and -dense enterocytes displayed similar ultrastructural characteristics. As in the jejunum, the nucleus of both cell types was situated in the basal region of the cell and there were many mitochondria in the apical cytoplasm (Fig. 1A,D). In the electron-lucid enterocytes, the cellular cytoplasm was more electron-lucid than the mitochondrial matrix while the cytoplasm of the dense enterocytes presented a similar electron-density than the mitochondrial matrix (Fig. 1D,E). Goblet cells exhibited numerous mucus granules, that distended the apical region of the cell, and cellular organelles, that were placed at their lateral and inferior margins (Fig. 2A–C). Several secreting goblet cells were observed (Fig. 2c), as well as goblet cells with intact mucus granules (Fig. 2A–C). Enteroendocrine cells were identified in the lower part of the crypts, recognizable by their basal and perinuclear region containing characteristic dense secretory granules (Fig. 2d,D). The granules varied considerably in shape (Fig. 2D). The Paneth cells were situated at the base of the Lieberkühn crypts in the two intestinal segments, with predominance in the jejunum. Of pyramidal shape, they exhibited a cytoplasm with numerous apical granules of variable electron density, a supranuclear Golgi apparatus and a very developed rough endoplasmic reticulum (Fig. 3A,a,B,b,F). Most of the secretory granules contained a homogeneous matrix of moderately high electron density; others showed a bipartite substructure with an electron-dense center and a peripheral region of lower density (Fig. 3C). The electron densities of the granules varied relatively from cell to cell and some Paneth cell granules exhibited crescent structures of high electron density (Fig. 3D). Several desmosomes (macula adherens) were observed between Paneth cells (Fig. 3E,F).

Conventional Histochemistry

Table 3 illustrates the histochemical analysis of the jejunum and ileum. In both regions, goblet cells exhibited carboxylated and sulfated GCs (Figs. 4A–C and 5A–C), GCs with oxidizable vicinal diols (Figs. 4D and 5D), GCs with sialic acid residues (Figs. 4F and 5G), and neutral sugars (Figs. 4G and 5H). Furthermore, the sequence AB pH 2.5/PAS allowed the identification of goblet cells PAS positive as well as a higher proportion of AB/PAS positive, both in the villus epithelium and in the glandular crypts (Figs. 4E and 5E,F). The TB technique at both pH values evidenced the presence of metachromatic goblet cells along the vertical crypt-villus axis of the jejunum and ileum (Figs. 4H,I and 5I,J).

Although the staining intensity of goblet cells was similar for most techniques, several methods showed remarkable variations according to the anatomical region studied. Histochemical results revealed the presence of carboxylated and sulfated GCs in both regions although sulfomucins were clearly prevalent in the ileum (Figs. 4B,C,I and 5B,C,J). Sialic acid was highly O-acetylated and was particularly abundant in the jejunum, while ileal goblet cells showed a slight staining with the PA/Bh/KOH/PAS sequence (Figs. 4F and 5G). The KOH/PA*/Bh/PAS technique evidenced a more intense histochemical reaction in the jejunal than in the ileum goblet cells, therefore demonstrating a reduction of neutral mucins in the distal small intestine (Figs. 4G and 5H).

In the glycosylation profile of the enterocytes and the glycocalyx, no differences were observed between regions.

Lectin Histochemistry

Table 4 summarizes the distribution of specific sugar residues in the jejunum and ileum of *L. maximus*. The lectin-histochemical study revealed a spatial variation in the glycosylation pattern of intestinal mucins, mainly in goblet cells. In both regions, these cells showed moderate to strong affinity for Con-A, PNA, and RCA-I and lower affinity for SBA (Figs. 6A–D and 7A–D). The binding pattern of the remaining lectins to the goblet cells varied according to the anatomical region. The labeling of these cells for WGA and UEA-I was stronger in the jejunum than in the ileum (Figs. 6E,e,F and 7E,F). Jejunal goblet cells stained moderately with DBA, while no affinity for this lectin was observed in the ileum (Figs. 6G and 7G,g).

In both regions, the Paneth cells were identified by their production of fucosylated glycans detected by lectin UEA-I (Figs. 6H and 7F).

Only in the jejunum, WGA and UEA-I binding was evident in the supranuclear area of the enterocytes probably corresponding to the Golgi complex (Fig. 6E,e,F). In these absorptive cells, no staining was observed with the other lectins.

The glycocalyx presented the same lectin binding pattern in both regions, exception made of WGA and PNA which were evident only in the jejunum (Figs. 6D,E,e and 7D,E).

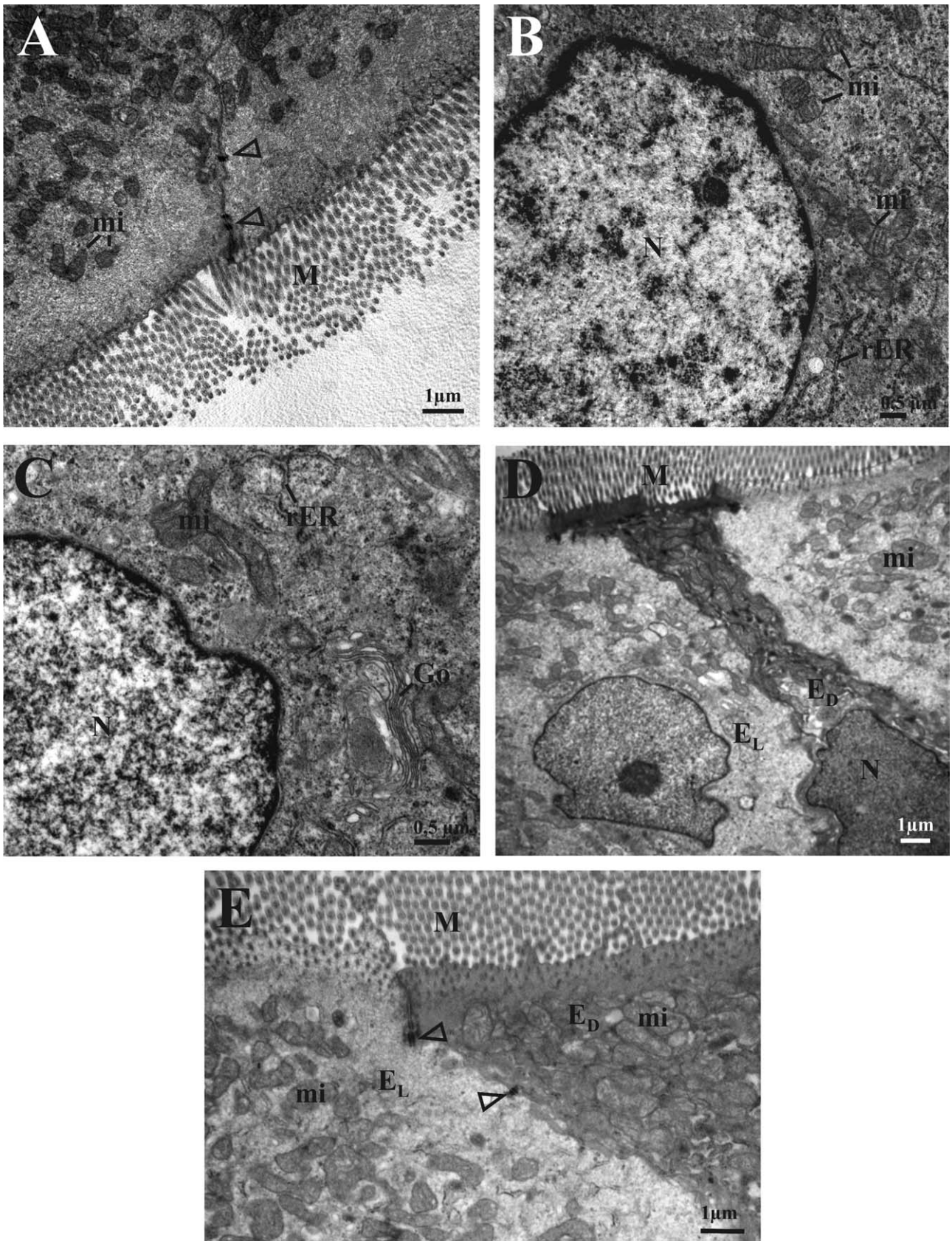

Fig. 1. Transmission electron micrographs of enterocytes. **(A)** Jejunal enterocytes, **(B, C)** perinuclear cytoplasm with cisterns of rough endoplasmic reticulum, a perinuclear Golgi apparatus and mitochondria, and **(D, E)** ileal enterocytes. Note the two morphological types of enterocytes recognizable by the different electron density of their cytoplasm. Arrowhead, junctional complex; E_D, electron-dense enterocyte; E_L, electron-lucid enterocyte; Go, Golgi; M, microvilli; mi, mitochondria; N, nucleus; rER, rough endoplasmic reticulum.

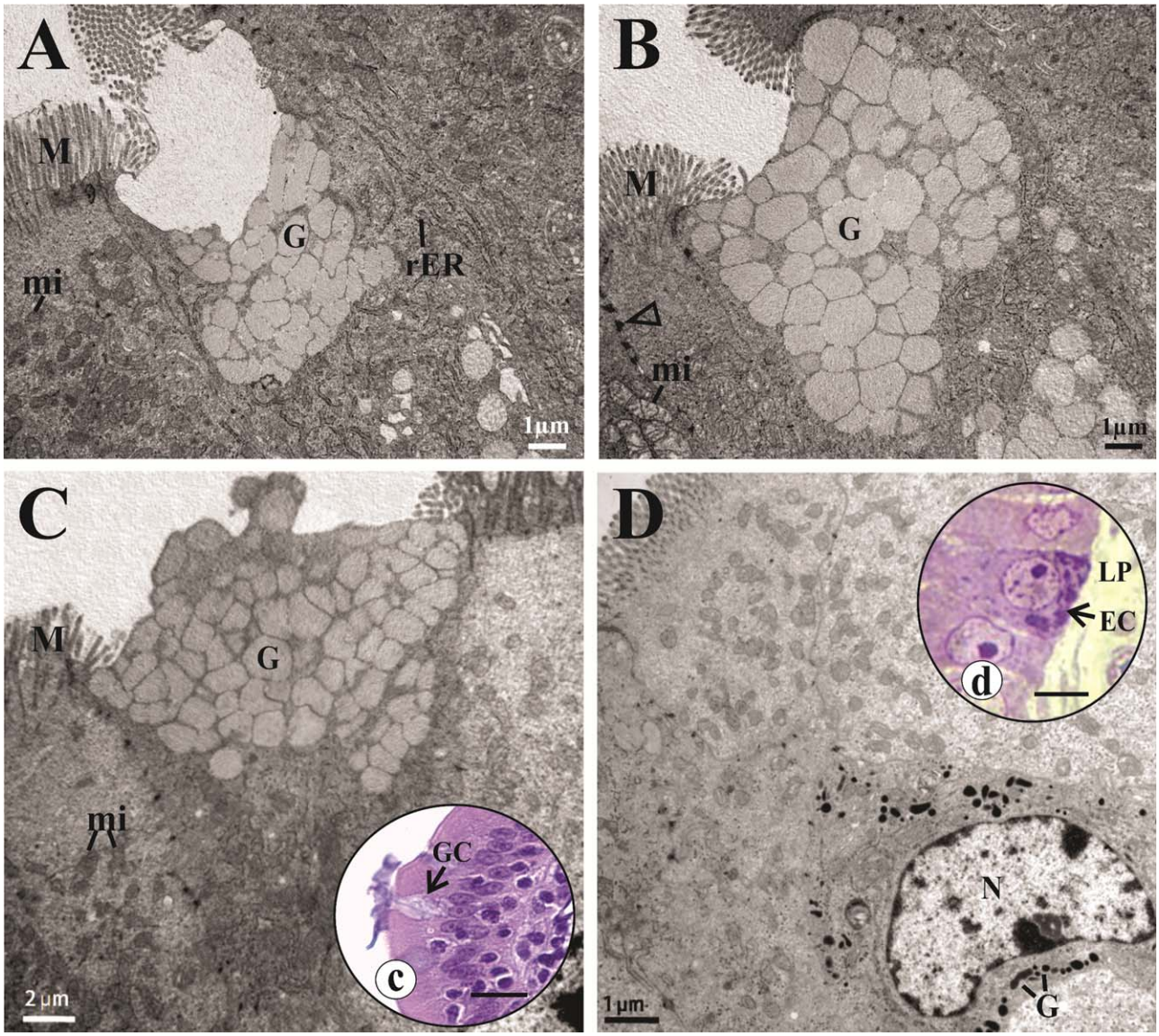

Fig. 2. Transmission electron micrographs of intestinal epithelial cells. **(A–C)** Goblet cells with numerous electron-lucid mucous granules distending the apical region of the cell. Image (c) shows the secreting goblet cell identified by hematoxylin and eosin stain, scale bar: 10 µm (light microscopy). **(D)** Endocrine cell with characteristic dense secretory granules in the basal and perinuclear region of the cell. Image (d) shows the details of the same cell identified in semithin section, scale bar: 10 µm (light microscopy, Toluidine Blue). Arrowhead, junctional complex; EC, Endocrine cell; G, secretory granules; GC, goblet cell; LP, lamina propria; M, microvilli; mi, mitochondria; N, nucleus; rER, rough endoplasmic reticulum.

DISCUSSION

In this study, we report a detailed histochemical analysis of the intestinal epithelial cells of *Lagostomus maximus* clearly showing different patterns of glycosylation between jejunum and ileum. Moreover, this study complements previous investigations on the digestive system of the plains viscacha and, in connection with our preceding paper, provides evidence for a region-specific glycopattern along the small intestine (Tano de la Hoz et al., 2014). The results obtained from the histochemical methods showed an increasing gradient of sulfomucins from duodenum to ileum, associated with a decreasing gradient of neutral mucins and O-acetylated sialic acid (Tano de la Hoz et al., 2014). These findings are in agreement with Boonzaier et al. (2013) and Robbe et al. (2004), who found the presence of an acidic gradient along the small and large intestine of several mammals. Regarding the functional implications of our findings, it can be hypothesized that the glycosylation pattern differences along the intestinal tract would be a responsive system capable of adapting to local physiological requirements, including response to bacterial colonization (Moran et al., 2011).

Recent studies on rodents have demonstrated that the gut microflora specifically modulates the intestinal glycosylation pattern by changing the cellular and subcellular distribution of glycans (Freitas et al., 2002; Moran

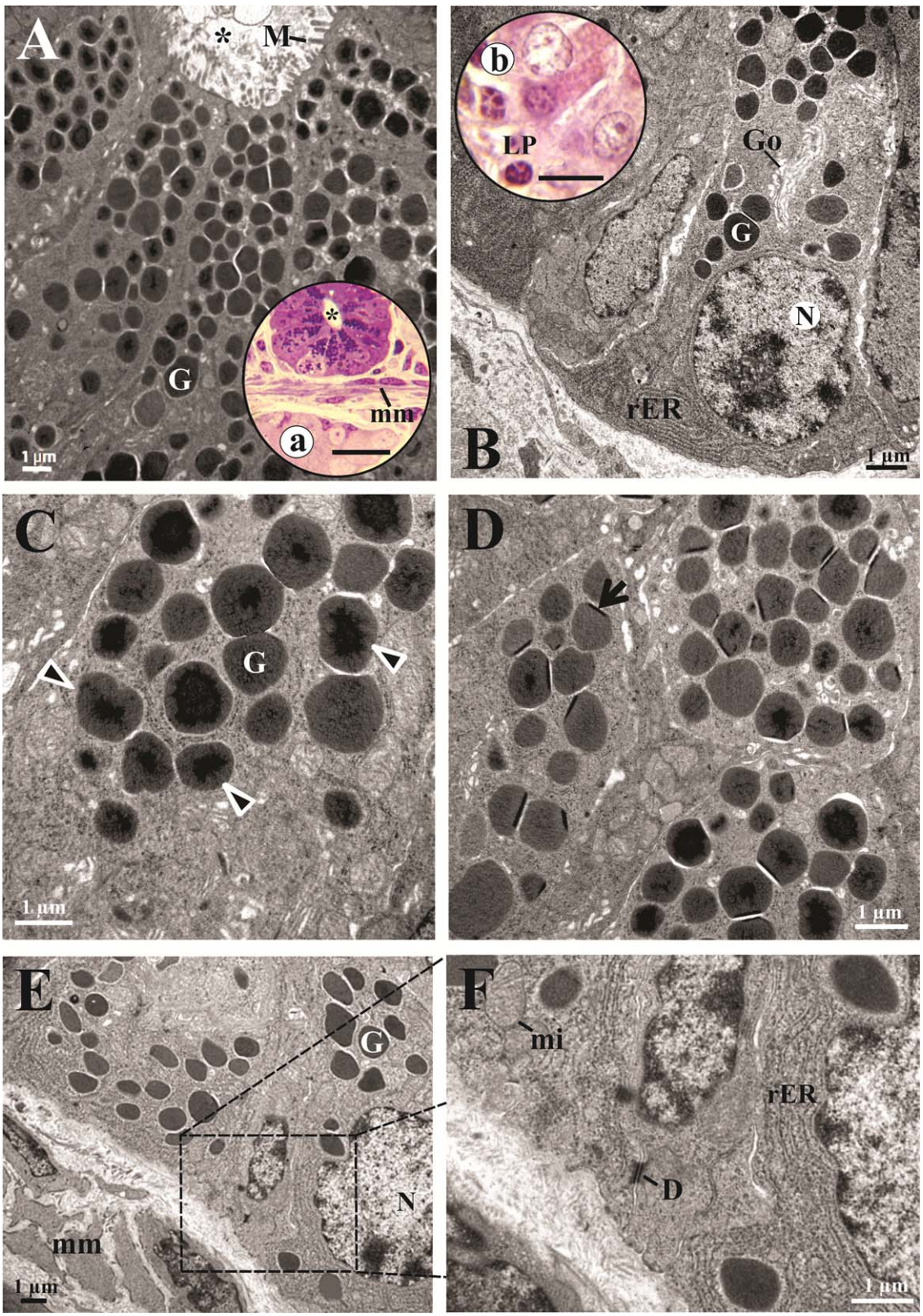

Fig. 3. Transmission electron micrographs of Paneth cells. **(A)** Paneth cells at the bottom of a crypt. Image (a) shows details of the same cells identified in semithin section, scale bar: 10 µm (light microscopy, Toluidine Blue). **(B)** Paneth cell with numerous apical cytoplasmatic granules. Image (b) shows the details of a Paneth cell identified by hematoxylin and eosin stain, scale bar: 10 µm (light microscopy). **(C)** High-magnification image from the apical region of a Paneth cell. Note the secretory granules with a bipartite substructure (arrowhead). **(D)** High-magnification image from the secretory granules. There are granules with crescent structures (arrow). **(E)** Basal region of Paneth cells. **(F)** Higher magnification of figure E. Asterisk, lumen; D, desmosome; G, secretory granules; Go, Golgi; LP, lamina propria; M, microvilli; mi, mitochondria; mm, muscularis mucosae; N, nucleus; rER, rough endoplasmic reticulum.

TABLE 3. Histochemical analysis of the jejunum and ileum of *Lagostomus maximus*

	Jejunum			Ileum		
Procedures	Glycocalyx	Enterocyte	Goblet cells	Glycocalyx	Enterocyte	Goblet cells
PAS	3	1	3	3	1	3
α-amylase/PAS	3	1	3	3	1	3
KOH/PA*S	2	1	2	2	1	2
PA/Bh/KOH/PAS	1	1	2	1	1	1
KOH/PA*/Bh/PAS	3	2	3	3	2	1
AB pH 2.5	2	0	0^a-3^b	2	0	0^a-3^b
AB pH 1.0	2	0	0^a-1^b	2	0	0^a-2^b
AB pH 0.5	1	0	0^a-1^b	1	0	0^a-2^b
AB pH 2.5/PAS	3P	1M	$3M^a-3P^b$	3P	1M	$3M^a-3P^b$
AB pH 1.0/PAS	3P	1M	$3M^a-3P^b$	3P	1M	$3M^a-3P^b$
TB pH 5.6	3or	3or	3m	0or	3or	3m
TB pH 4.2	0or	1or	1m	0or	1or	2m

m, metachromasia; M, magenta; or, ortochromasia; P, purple.
Staining intensity: 0, negative; 1, slightly positive; 2, moderate; 3, strong.
[a],[b]Goblet cells with two different histochemical profiles were differentiated.

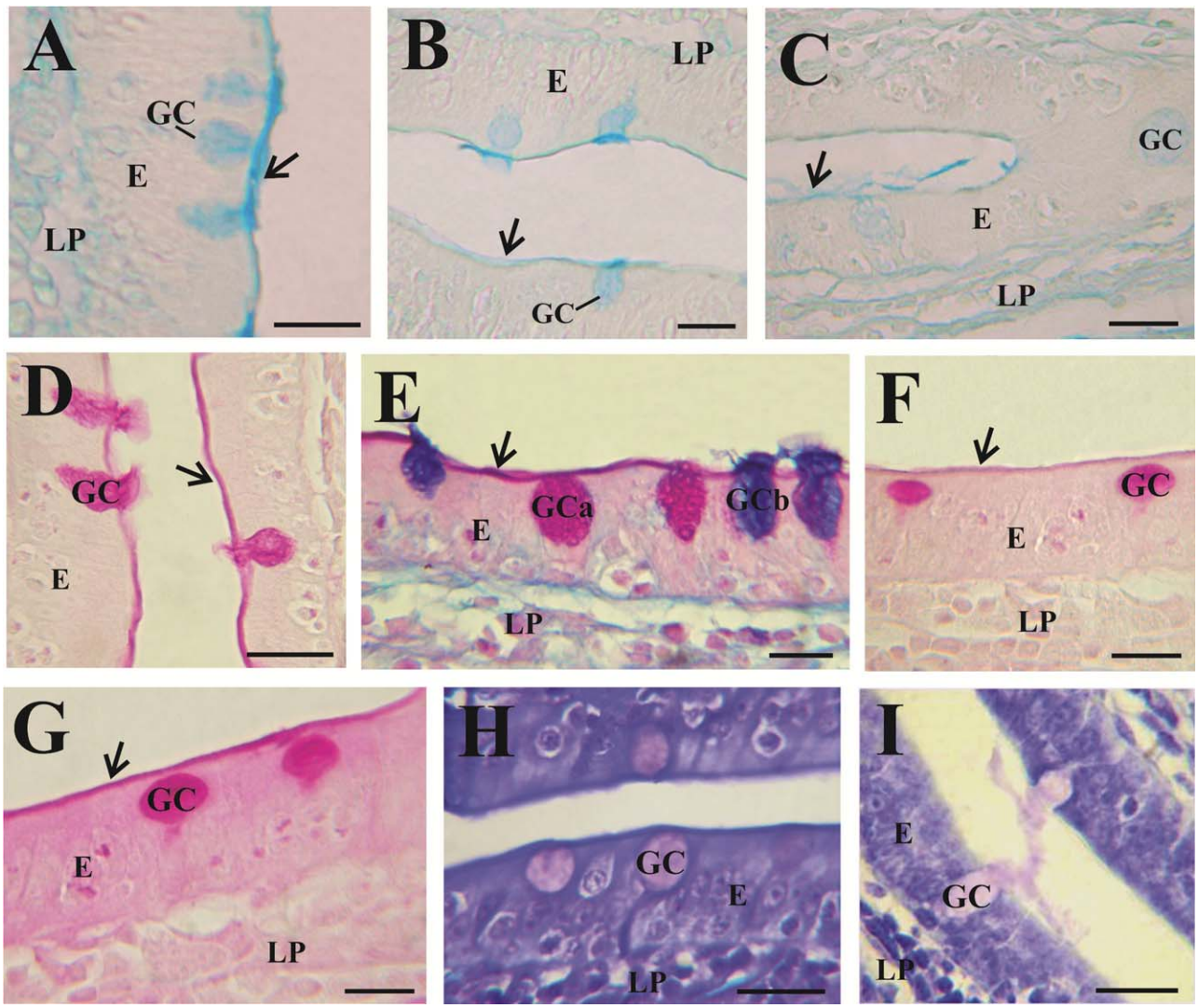

Fig. 4. Histochemical characterization of glycoconjugates in the jejunal epithelium. **(A)** AB pH 2.5, **(B)** AB pH 1.0, **(C)** AB pH 0.5, **(D)** PAS, (**E)** AB pH 2.5/PAS, **(F)** PA/Bh/KOH/PAS, **(G)** KOH/PA*/Bh/PAS, **(H)** AT pH 5.6, and **(I)** AT pH 4.2. E, epithelial layer; GC, goblet cell; GC_a, goblet cell PAS positive; GC_b, goblet cell AB/PAS positive; LP, lamina propria; arrow, glycocalyx. Scale bars: 5 μm (A, B, E, F, G) and 10 μm (C, D, H, I).

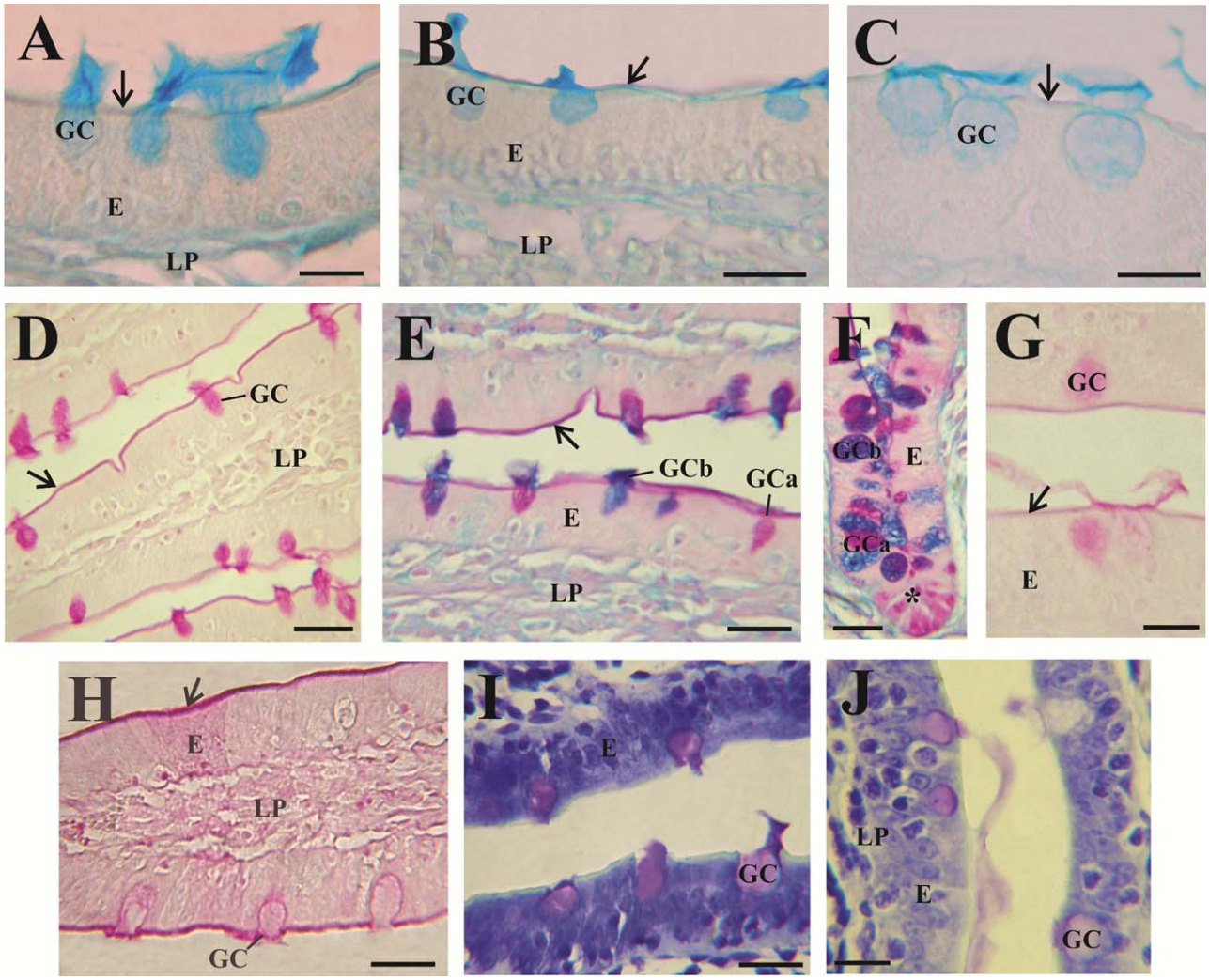

Fig. 5. Histochemical characterization of glycoconjugates in the ilial epithelium. **(A)** AB pH 2.5, **(B)** AB pH 1.0, **(C)** AB pH 0.5, **(D)** PAS, **(E, F)** AB pH 2.5/PAS, **(G)** PA/Bh/KOH/PAS, **(H)** KOH/PA*/Bh/PAS, **(I)** AT pH 5.6, and **(J)** AT pH 4.2. E, epithelial layer; GC, goblet cell; GC_a, goblet cell PAS positive; GC_b, goblet cell AB/PAS positive; LP, lamina propria; arrow, glycocalyx; asterisk, Paneth cell. Scale bars: 5 μm (A, C, G, H) and 10 μm (B, D–F, I, J).

et al., 2011). The presence of large numbers of microorganisms is generally related with the secretion of sulfated mucin. Some studies have shown that sulphomucins are resistant to degradation by bacterial glycosidases and have a strong inhibitory effect on bacterial growth. Indeed, it has been shown that enzymatic desulfation of colon mucus greatly increases its susceptibility to the degradation by fecal glycosidases (Rhodes et al., 1985). In this study, the histochemical results showed the existence of sulfomucins and sialomucins along the small intestine of *L. maximus* (Tano de la Hoz et al., 2014), although sulfomucins were clearly prevalent in the ileum. In view of the fact that the amount of bacteria increases throughout the intestinal tube (Pelaseyed et al., 2014), the acidic gradient found along the small intestine of the viscacha would be related to microbial population differences of the regions.

It is known that in mammals, the negative charge of mucins is due to the content of sialic acid and sulfated residues (Pastoriza and Hulen, 2006). In *L. maximus*, sialic acid was highly O-acetylated and was particularly abundant in the jejunum, while ileal goblet cells showed a slight staining with the PA/Bh/KOH/PAS technique. Several authors have demonstrated that the degree of acetylation of sialomucins may influence the efficacy of the protective action against the mucus bacterial degradation because the substituent groups represent a steric effect (Mastrodonato et al., 2013, 2014). Therefore, assuming that the sialic acid acetylation enhances the resistance to bacterial breakdown of glycans (Mastrodonato et al., 2013), it can be hypothesized that the decrease in staining intensity of goblet cells with the PA/Bh/KOH/PAS technique in the ileum of the viscacha could reduce the resistance of these mucins against bacterial sialidase; nevertheless, the protective role in this intestinal region could probably be played by highly sulfated mucins. Previous studies have demonstrated that the presence of sulfate groups in an oligosaccharide

TABLE 4. Lectin histochemical analysis of jejunum and ileum of *Lagostomus maximus*

		Jejunum	Ileum
Con-A	*Glycocalyx*	3	3
	Enterocyte	1	1
	Goblet cells	2	2
WGA	*Glycocalyx*	3	0
	Enterocyte	1[a]	0
	Goblet cells	2	1
DBA	*Glycocalyx*	0	0
	Enterocyte	0	0
	Goblet cells	1	0
SBA	*Glycocalyx*	0	0
	Enterocyte	0	0
	Goblet cells	1	1
RCA-I	*Glycocalyx*	3	3
	Enterocyte	0	1
	Goblet cells	2	2
PNA	*Glycocalyx*	3	0
	Enterocyte	0	0
	Goblet cells	3	3
UEA-I	*Glycocalyx*	3	3
	Enterocyte	1[a]	0
	Goblet cells	2	1

Staining intensity: 0, negative; 1, slightly positive; 2, moderate; 3, strong.
[a]Only the supranuclear region of the enterocytes was labeled.

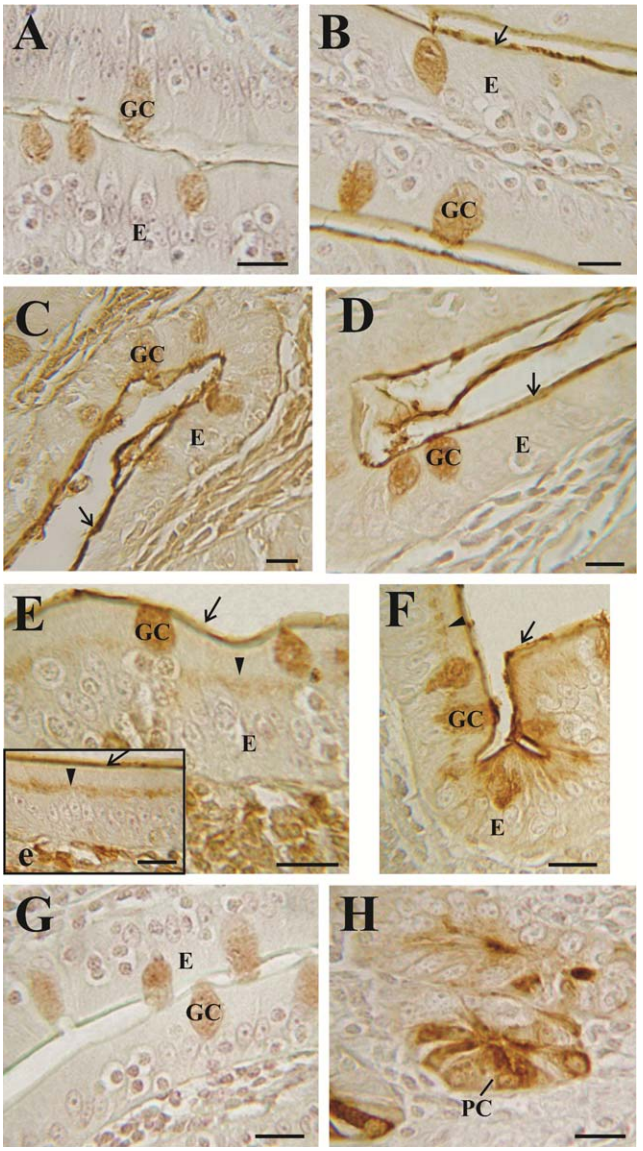

Fig. 6. Lectin binding profile of the jejunum. **(A)** Lectin SBA, (**B**) Lectin RCA-I, **(C)** Lectin Con-A, **(D)** Lectina PNA, **(E, e)** Lectin WGA, (**F**) Lectin UEA-I, **(G)** Lectin DBA, and (**H**) Paneth cells were identified by their production of fucosylated glycans detected by lectin UEA-I. E, epithelial layer; GC, goblet cell; PC, Paneth cell; arrow, glycocalyx; arrowhead, supranuclear granules. Scale bar: 5 μm.

chain can interfere with lectin–sugar interactions (Menarguez-Martinez et al., 1992; Parillo et al., 2001). In this study, some differences were detected between the histochemical and lectin-histochemical results. Thus, it was shown that intestinal goblet cells of both regions have a similar reaction with KOH/PA*S technique but not with WGA, being the latter lower in the ileum. Also, the glycocalyx of the ileum, that should have sialic acid residues as was revealed by histochemical method, was negative to WGA binding. Given the high sulfation of the ileal mucins, the differences observed between the KOH/PA*S technique and WGA could be due to a strong inhibition of the lectin–sugar interactions by the sulfate groups present in the GCs. Thus, our results might indicate that in the ileum WGA binding is possibly inhibited by the high sulfation of terminal sialic acid residues. These results are consistent with other studies in rodents which have shown a higher labeling intensity of certain lectins, including WGA, after a pretreatment desulfation (Liquori et al, 2012; Mastrodonato et al, 2013, 2014; Scillitani and Mentino, 2015). Lectin-histochemical methods combined with chemical and enzymatic treatments could be used in future studies to confirm the presence of highly sulfated sialic acid residues in the ileum of *L. maximus*.

As a large proportion of secreted mucins are synthesized and stored in unicellular epithelial glands, the goblet cells, considerable interest has been directed to their function, glycopattern, and morphology (McDole et al., 2012). Some studies have shown that the glycosylation pattern of goblet cells varies along the vertical crypt-villus axis (Galotta et al., 2009). Also, Liquori et al. (2012) showed that the distribution of sialomucins and sulfomucins differ along the intestinal crypt of the mouse colon, which suggests that the distribution patterns found in the crypts could be associated with goblet cells in different maturation stages. However, our results showed no significant difference between the crypts and the intestinal villi goblet cells, thus concluding that in the small intestine of *L. maximus*, as in other rodent species (Boonzaier et al., 2013), no glycosylation patterns along the crypt–villus axis that could be associated to the state of maturation of the goblet cells were evident. By the sequence AB pH 2.5/PAS, we identified goblet cells with two different histochemical profiles, being the mixed mucins secreting goblet cells the larger type in the small intestine of *L. maximus*. These finding correlated with the work of Boonzaier et al. (2013) who studied the distribution of mucin goblet cells in the gastrointestinal tract of three mammalian species.

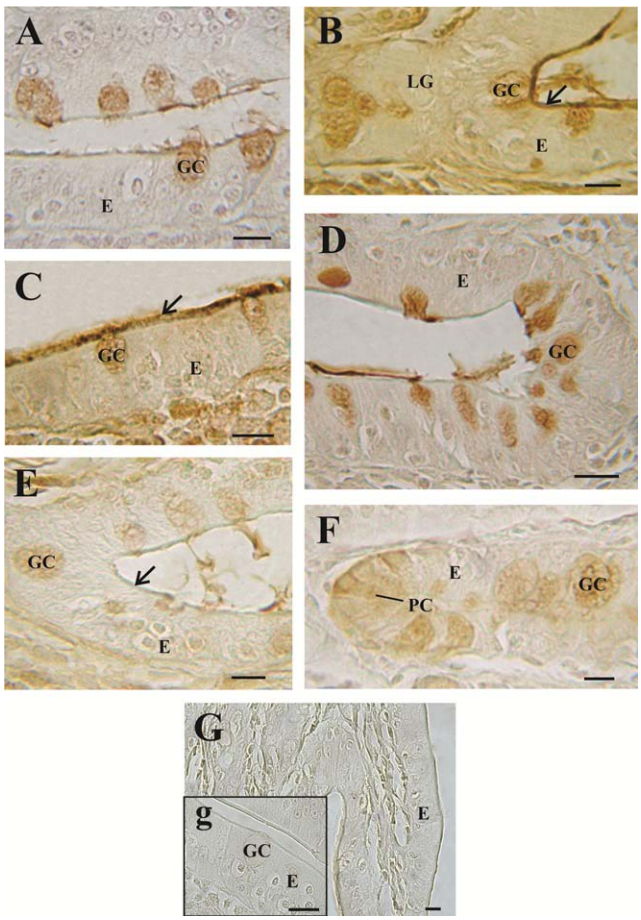

Fig. 7. Lectin binding profile of the ileum. **(A)** Lectin SBA, **(B)** Lectin RCA-I, **(C)** Lectin Con-A, **(D)** Lectin PNA, **(E)** Lectin WGA, **(F)** Paneth cells were identified by their production of fucosylated glycans detected by lectin UEA-I, and **(G, g)** Lectin DBA. E, epithelial layer; GC, goblet cell; LG, Lieberkühn gland; PC, Paneth cell; arrow, glycocalyx. Scale bar: 5 μm.

Tootian et al. (2013) obtained similar results using histochemical techniques in different portions of the Persian squirrel, *Sciurus anomalus*, small intestine. These similarities between distantly related species suggest that neutral and acid mucin types are essential to most mammals, irrespective of their taxonomy.

Lectin-histochemistry represents a useful tool that allows the identification and localization of terminal and subterminal residues of the glycosidic chains of mucins (Mastrodonato et al., 2014). L-fucose is usually presented in many N- and O-linked glycans and it is related with the mucus viscosity (Liquori et al., 2012). In the goblet cells, the UEA-I binding pattern was strongly dependent on the intestinal segment and showed a *L. maximus* fucose reduction from duodenum to ileum (Tano de la Hoz et al., 2014). These results are similar to those obtained by Robbe et al. (2004) who showed the presence of a decreasing gradient of fucose of humans throughout the intestinal tract. Also, Freitas et al. (2002) found a similar fucosylation pattern in mice ileum and colon, suggesting a downregulation of fucosyltransferases in these levels. In this study, WGA binding was mainly observed in the jejunum, and showed the existence of glycans with GlcNAc residues in goblet cells, glycocalyx and a cytoplasmatic area probably corresponding to the Golgi apparatus of the enterocytes. In mammals, the presence of GalNAc has been particularly important in relation to mucin acidification (Liquori et al., 2012).

The morphology and ultrastructure of the small intestine have been studied in a large number of species (Satoh et al., 1990; Leis et al., 1997; Hosoyamada and Sakai, 2007; Zanuzzi et al., 2008; Hansen and Rasmussen, 2009; Mantani et al., 2014; Vásquez Cachay et al., 2014). From these studies, it is well known that some morphological features are shared by mammals, whereas some others are particular of each species.

Thus, several works have demonstrated that Paneth cells show morphological diversity between species; it has been observed principally that the apical granules vary in size, number, and ultrastructure (Satoh et al., 1990). The Paneth cells of guinea pigs showed granules with homogeneous electron-dense content, while golden hamsters evidenced granules of varying electron density. Unlike those rodents, viscacha Paneth cell granules contained a homogeneous matrix of relatively high electron density, but other granules showed bipartite substructure having an electron-dense center and a peripheral region of lower density. Since several differences were observed in the granules ultrastructure even between related species, it is probable that the ultrastructural characteristics of the Paneth cells granules are not related to the phylogenetic classification.

It is important to note that the bipartite substructure found in the viscacha Paneth cell granules had similar characteristics to those described in other mammals, including mice, rats, and humans. Besides, Leis et al. (1997) demonstrated that the secretory granules of the rat Paneth cells were composed of an electron-lucid peripheral halo containing O-linked oligosaccharides with N-acetyl galactosamine and N-acetyl glucosamine residues, and an electron-dense core containing N- and O-linked oligosaccharides with fucose residues. This ultrastructural cytochemical study enables us to suggest that in *L. maximus* the biphasic structure observed in Paneth cell granules could be a consequence of their cytochemical composition. Indeed, the lectin binding pattern of rat, mouse, and rabbit Paneth cells granules is in accordance with the glycopattern found in *L. maximus*, in which Paneth cells granules presented fucose residues both in the jejunum and the ileum (Leis et al., 1997; Zanuzzi et al., 2008). The presence of similar oligosaccharides in the glycoprotein composition of Paneth cell granules across different species suggest that these are constitutively expressed conserved glycoproteins.

Comparing the ultrastructural characteristics of the jejunum and ileum, only differences in absorptive cells or enterocytes were observed. In the ileum, two types of enterocytes were recognized based on the electron density of the cytoplasm; the largest cell type had electron-lucid cytoplasm; the other cell type had electron-dense cytoplasm. Similar results were reported in previous vertebrate studies, in which two-type enterocytes differing in the cytoplasm density had been observed (Korneva and Bednyakov, 2011). Although we found no particular spatial distribution in these cell types, our results could give structural or morphological support to previous studies on the human small intestine; they have

provided evidence for the existence of two types of enterocytes at the molecular level characterized by differences in their gene profile and their spatial distribution within the crypt–villus axis (Gassler et al., 2006). Thus, it is probable that the presence of two types of enterocytes in *L. maximus* could be related to different physiological states.

In conclusion, even though the intestinal epithelium of *Lagostomus maximus* exhibited ultrastructural characteristics similar to those of other rodents, it also showed features particular of the species, such as the structural complexity of the Paneth cell granules and the presence of two types of enterocytes that differ in cytoplasmic density.

Moreover, this study showed important variations in the mucin-associated oligosaccharide content with an increasing gradient of sulfomucins from duodenum to ileum, associated with a decreasing gradient of neutral mucins, O-acetylated sialic acid, and fucose residues (Tano de la Hoz et al., 2014). These data show that mucin glycosylation varies according to different anatomical regions and probably constitutes a responsive system adapted to local physiological requirements (Moran et al., 2011). Our results show significant information for future histochemical analysis to assess changes in the glycosylation pattern of intestinal mucins under different feeding conditions.

ACKNOWLEDGEMENT

The authors thank the staff of the Estación de Cría de Animales Silvestres (ECAS), Ministerio de Asuntos Agrarios de la Provincia de Buenos Aires.

LITERATURE CITED

Addo P, Dodoo A, Adjei S, Awumbila B. 2003. Optimal duration of male-female exposure to optimize conception in the grasscutter (*Thryonomys swinderianus*). Livest Res Rural Dev 15.

Bansil R, Turner BS. 2006. Mucin structure, aggregation, physiological functions and biomedical applications. Curr Opin Colloid Interface Sci 11:164–170.

Beyaz F, Liman N. 2009. The prenatal development and histochemistry of the ileal mucins in the bovine fetuses. Anat Histol Embryol 38:436–442.

Boonzaier J, Van der Merwe EL, Bennett NC, Kotze SH. 2013. Comparative gastrointestinal morphology of three small mammalian insectivores: *Acomys spinosissimus* (Rodentia), *Crocidura cyanea* (Eulipotyphla), and *Amblysomus hottentotus* (Afrosoricida). J Morphol 274:615–626.

Commission on Life Sciences National Research Council. 1996. Institute of Laboratory Animals Resources. Guide for the care and use of laboratory animals. Washington DC: National Academic Press.

Culling CFA, Reid PE, Dunn WL. 1976. A new histochemical method for the identification and visualization of both side-chain acylated and non-acylated sialic acids. J Histochem Cytochem 24: 1225–1230.

Edderai D, Ntsame M, Houben P. 2001. Gestion de la reproduction en aulacodiculture. Synthèse des outils et méthodes existants. INRA Prod Anim 14:97–103.

Freitas M, Axelsson LG, Cayuela C, Midtvedt T, Trugnan G. 2002. Microbial–host interactions specifically control the glycosylation pattern in intestinal mouse mucosa. Histochem Cell Biol 118:149–161.

Galotta JM, Márquez SG, Zanuzzi CN, Gimeno EJ, Portiansky EL, Barbeito CG. 2009. Lectin binding pattern of intestinal goblet cell in horse, pig and rabbit. Animal Biology Journal 1:49–55.

Gassler N, Newrzella D, Böhm C, Lyer S, Li L, Sorgenfrei O, van Laer L, Sido B, Mollenhauer J, Poustka A, Schirmacher P, Gretz N. 2006. Molecular characterisation of non-absorptive and absorptive enterocytes in human small intestine. Gut 55:1084–1089.

Hansen GH, Rasmussen K. 2009. Lipopolysaccharide-binding protein: localization in secretory granules of Paneth cells in the mouse small intestine. Histochem Cell Biol 131:727–732.

Hosoyamada Y, Sakai T. 2007. Mechanical components of rat intestinal villi as revealed by ultrastructural analysis with special reference to the axial smooth muscle cells in the villi. Arch Histol Cytol 70:107–116.

Jackson JE. 1985. Ingestión voluntaria y digestibilidad en la vizcacha (*L. maximus*). Rev Arg Prod Anim 5:113–119.

Kim YS, Ho SB. 2010. Intestinal goblet cells and mucins in health and disease: recent insights and progress. Curr Gastroenterol Rep 12:319–330.

Korneva ZV, Bednyakov DA. 2011. Comparative characterization of the ultrastructure of intestinal epithelium of various sturgeon species. Inland Water Biol 4:446–454.

Leis O, Madrid JF, Ballesta J, Hernández F. 1997. N- and O-linked oligosaccharides in the secretory granules of rat Paneth cells: an ultrastructural cytochemical study. J Histochem Cytochem 45: 285–293.

Lev RA, Spicer SS. 1964. Specific staining of sulphate groups with Alcian Blue at low pH. J Histochem Cytochem 12:309.

Liquori GE, Mastrodonato M, Mentino D, Scillitani G, Desantis S, Portincasa P, Ferri D. 2012. *In situ* characterization of O-linked glycans of Muc2 in mouse colon. Acta Histochem 114:723–732.

Lison L. 1953. Histochimie et cytochimie animales. Principes et méthodes. Paris: Gauthier-Villars.

Llanos AC, Crespo JA. 1952. Ecología de la vizcacha (*Lagostomus maximus maximus* Blainville) en el nordeste de la provincia de Entre Ríos. R Inv Agr 3:289–378.

Mantani Y, Nishida M, Yuasa H, Yamamoto K, Takahara EI, Omotehara T, Sanath Udayanga KG, Kawano J, Yokoyama T, Hoshi N, et al. 2014. Ultrastructural and histochemical study on the Paneth cells in the rat ascending colon. Anat Rec 295:1462–1471.

Martinez-Menarguez JA, Ballesta J, Aviles M, Madrid JF, Castells MT. 1992. Influence of sulphate groups in the binding of peanut agglutinin. Histochemical demonstration with light- and electron-microscopy. Histochem J 24:207–216.

Mastrodonato M, Mentino D, Liquori GE, Ferri D. 2013. Histochemical characterization of sialic acid residues in mouse colon mucins. Microsc Res Tech 76:156–162.

Mastrodonato M, Mentino D, Portincasa P, Calamita G, Liquori GE, Ferri D. 2014. High-fat diet alters the oligosaccharide chains of colon mucins. Histochem Cell Biol 142:449–459.

Mc Manus JFA. 1948. Histological and histochemical uses of periodic acid. Stain Technol 23:99–108.

McDole JR, Wheeler LW, McDonald KG, Wang B, Konjufca V, et al. 2012. Goblet cells deliver luminal antigen to CD103+ dendritic cells in the small intestine. Nature 483:345–349.

Moran AP, Gupta A, Joshi L. 2011. Sweet-talk role of host glycosylation in bacterial pathogenesis of the gastrointestinal tract. Gut 60:1412–1425.

Mowry RW. 1963. The special value of methods that colour both acidic and vicinal hydroxyl groups in the histochemical study of mucins with revised directions for the colloidal iron stain, the use of Alcian blue 8GX, and their combination with the periodic acid-Schiff reaction. Ann N Y Acad Sci 106:402–423.

National Research Council (USA). 2000. Coypu. In: Vietmeyer N, editor. Microlivestock: little-known small animals with a promising economic future. Washington DC: Office of International Affairs (OIA), National Academy Press. p 217–224.

Neutra MR, Forstner JF. 1987. Gastrointestinal mucus: synthesis, secretions, and function. In: Johnson LR, editor. Physiology of the gastrointestinal tract. NewYork: Raven Press. p 975–1009.

Parillo F, Diverio S, Todini L, Fagioli O. 2001. Histochemical detection of the lectin-binding carbohydrates in the zona pellucida during oocyte growth in the wild boar (*Sus scrofa scrofa*). Vet Res 32: 581–590.

Pastoriza GM, Hulen C. 2006. Influence of sialic acid and bacterial sialidase on differential adhesion of *Pseudomonas aeruginosa* to epithelial cells. Colloids Surf B 52:154–156.

Pearse AGE. 1985. Histochemistry: theoretical and applied, Vol. 2. Edinburgh: Churchill Livingstone.

Pelaseyed T, Bergström JH, Gustafsson JK, Ermund A, Birchenough GMH, Schütte A, van der Post S, Svensson F, Rodríguez-Piñeiro AM, Nyström EEL, et al. 2014. The mucus and mucins of the goblet cells and enterocytes provide the first defense line of the gastrointestinal tract and interact with the immune system. Immunol Rev 260:8–20.

Reid PE, Culling CFA, Dunn WL. 1973. Saponification induced increase in the periodic acid Schiff reaction in the gastrointestinal tract. Mechanism and distribution of the reactive substance. J Histochem Cytochem 21:473–483.

Rhodes JM, Gallimore R, Elias E, Allan RN, Kennedy JF. 1985. Faecal mucus degrading glycosidases in ulcerative colitis and Crohn's disease. Gut 26:761–765.

Robbe C, Capon C, Coddeville B, Michalski JC. 2004. Structural diversity and specific distribution of O-glycans in normal human mucins along the intestinal tract. Biochem J 384:307–316.

Satoh Y, Yamano M, Matsuda M, Ono K. 1990. Ultrastructure of Paneth cells in the intestine of various mammals. J Electron Micr Tech 16:69–80.

Scillitani G, Mentino D. 2015. Comparative glycopattern analysis of mucins in the Brunner's glands of the guinea-pig and the house mouse (Rodentia). Acta Histochem 117:612–623.

Tano de la Hoz MF, Flamini MA, Díaz AO. 2014. Histological and histochemical study of the duodenum of the plains viscacha (*Lagostomus maximus*) at different stages of its ontogenetic development. Acta Zool 95:21–35.

Tootian Z, Sadeghinezhad J, Sheibani MT, Fazelipour S, De Sordi N, Chiocchetti R. 2013. Histological and mucin histochemical study of the small intestine of the Persian squirrel (*Sciurus anomalus*). Anat Sci Int 88:38–45.

Vásquez Cachay ME, Pebe Gomez E, Rodriguez Gutierrez JL, Lira Mejia B, Falcón Pérez N, Zanuzzi CN, Barbeito C. 2014. Paneth cell identification in the small intestine of guinea pig offsprings (*Cavia porcellus*). Anat Rec 297:856–863.

Volz D, Reid PE, Park CM, Owen DA, Dunn WL. 1987. A new histochemical method for the selective periodate oxidation of total tissue sialic acids. Histochem J 19:311–318.

Zanuzzi CN, Fontana PA, Barbeito CG, Portiansky EL, Gimeno EJ. 2008. Paneth cells: histochemical and morphometric study in control and *Solanum glaucophyllum* intoxicated rabbits. Eur J Histochem 52:93–100.

Zuñiga M, Tur Marí J, Milocco S, Piñeiro R. 2001. Ciencia y Tecnología en Protección y Experimentación Animal. Aravaca: Mc Graw-Hill Interamericana.